RESEARCH PAPER

PCCP
www.rsc.org/pccp

In-situ spectroscopic investigations of surfactant adsorption and water structure at the CaF_2/aqueous solution interface†

Kevin A. Becraft,[a] Fred G. Moore[b] and Geraldine L. Richmond*[a]

[a] *Department of Chemistry, University of Oregon, Eugene, OR 97403-1253, USA E-mail: richmond@oregon.uoregon.edu.; Fax: 541-346-5859*
[b] *Department of Physics, Whitman College, Walla Walla, WA 99362-2083, USA*

Received 27th October 2003, Accepted 13th February 2004
First published as an Advance Article on the web 22nd March 2004

We report *in-situ* spectroscopic measurements of the structure and orientation of molecules in the interfacial region between the semi-soluble ionic solid CaF_2 (fluorite) and an aqueous phase. This paper integrates a series of new experiments with earlier results to give a comprehensive understanding of this very dynamic interface. We employ the surface specific technique, vibrational sum-frequency spectroscopy (VSFS), to study the effect that alterations in the aqueous phase composition, such as pH, surfactant ion concentration, and ion composition have on the bonding interactions, ion exchange behavior, and electrical properties in the interfacial region. These studies demonstrate the complex nature of the interactions of semi-soluble solids with an aqueous phase and the complexity of the surfactant adsorption process. Fundamental studies such as these are essential for understanding the mechanisms involved in surfactant adsorption and interfacial charge reversal; information which is important for industrially relevant processes such as mineral ore flotation, waste processing and petroleum recovery.

Introduction

The alteration and control of the surface properties of solids immersed in an aqueous phase is important to many diverse fields including oil recovery, colloidal stabilization, waste processing, and mineral ore separations *via* froth flotation.[1–3] In these and other applications, changes in the aqueous phase composition through the adjustment of pH, ionic strength, and concentration and type of surface active agents are used to control a variety properties of the solid surface. These properties include the solubilization of surface ions, passivation or activation of surface charge, alterations to the surface hydrophobicity, and changes in the chemical reactivity of the solid phase. Although much research has been devoted to insoluble oxide surfaces, relatively few studies have examined the changes that occur at ionic (salt-type) and semi-soluble solid surfaces. Salts, such as calcium fluoride (CaF_2, fluorite), tend to be much more soluble than mineral oxide and other covalent solids. Because of this relatively high solubility, these salts show very dynamic behavior in their surface properties when immersed in an aqueous phase. It is therefore important to know how this behavior manifests itself in alterations of the electrical properties of the surface, the adsorption of surfactant ions onto the surface, and the effect on the bonding and orientational behavior of interfacial water molecules comprising the aqueous interphase region.

Research conducted on the aqueous phase behavior of semi-soluble salt surfaces is generally carried out by contacting high surface area powders with a solution phase and monitoring changes in bulk ion concentration or mobility. Experiments of this type include potentiometric titrations,[4] zeta potential measurements,[5] IR spectroscopy,[6,7] and bulk adsorption studies.[8–11] These measurements are useful in studying bulk properties such as solubility and macroscopic adsorption of ions onto the salt surface, but cannot give molecular level information about the interfacial region. Other types of experiments such as FTIR-IRS,[12,13] contact angle measurements,[13,14] and infrared reflectance spectroscopy (DRIFT)[15,16] can monitor directly or extrapolate molecular level information, but they probe more than just the molecules in the interfacial region. In contrast, vibrational sum-frequency spectroscopy (VSFS) is a surface specific technique that gives molecular level information for a variety of interfacial species, including water molecules, while not relying on removal of large contributions from the vast number of molecules in the bulk. VSFS has been employed previously by our group to examine the CaF_2/solution interface.[17–19] These earlier studies demonstrate the sensitivity of VSFS to examine water structure[18] and surfactant adsorption processes[19] at the CaF_2/H_2O interface and introduced methods for deconvolution of the resulting complex VSFS spectra obtained.[17]

To obtain a more complete understanding of the interactions present at the CaF_2/aqueous interface and the adsorptive behavior of surfactants to that interface, we have pursued further detailed studies of CaF_2 immersed in a D_2O environment. Experiments were conducted over a wide range of surfactant concentrations and under two different polarization schemes. These D_2O studies clarify the complex spectral interferences arising between OH stretching modes of interfacial water molecules and the CH oscillators comprising the adsorbed surfactant tails. This new data, along with the integration and further analysis of data from the previous studies from our laboratory, provides a detailed picture of the semi-soluble salt, CaF_2 (fluorite), and the affect that alterations in pH and adsorption of surfactant ions have on the structure and orientation of molecules in the interfacial region. This type of information will help to enhance the understanding and predictability of processes such as surfactant adsorption and ion exchange behavior of salt type materials which are of fundamental and practical interest.

† Presented at the 81st International Bunsen Discussion Meeting on "Interfacial Water in Chemistry and Biology", Velen, Germany, September 19–23, 2003.

DOI: 10.1039/b313513f

Experimental

Experiments were conducted using a diode pumped Nd:YAG laser (Coherent, Infinity-100) producing 3.5 ns pulses at a repetition rate of 20 Hz. The fixed frequency fundamental 1.064 μm output is split into two beams: one passing through a BBO crystal to generate a fixed frequency 532 nm beam, the other passing through an optical parametric oscillator/optical parametric amplifier (OPO/OPA) system to generate an IR beam tunable from 2500–4000 cm^{-1} with a bandwidth of ~2 cm^{-1}. Complete details of the laser system may be found elsewhere.[20] The experimental sample cell consists of a hollow cylinder of Kel-F placed over the top of a large CaF_2 prism (ISP Optics) and sealed with an O-ring.[18] The sample cell is then filled with ~50 mL of aqueous solution, with the largest face of the prism (50 × 50 mm) used as the solid substrate. Additions to the sample cell were made *via* a micropipette with constant stirring provided by a mechanical stirring paddle. The visible and IR beams were directed towards the interface at incident angles at, or slightly above, their respective critical angles; this total internal reflection (TIR) geometry greatly enhances the sum-frequency response over externally reflected set-up geometries.[21] The sum-frequency signal generated from the interface was collected *via* a PMT detector and gated electronics after passing through several filters to remove stray light and the reflected fundamental beams. All data were normalized to fluctuations of the IR power. Spectra were obtained using the following two polarization schemes: SSP (sum-frequency (s), visible (s), and IR (p)) which probes dipole transition moments with components normal to the plane of the interface; and SPS (sum-frequency (s), visible (p), and IR (s)) which probes dipole transition moments with components parallel to the plane of the interface. The CaF_2 prism required periodic cleaning, which was carried out by quickly dipping the prism in a solution of concentrated sulfuric acid containing NoChromix, followed by copious rinsing in water. It was occasionally necessary to polish the prism after prolonged exposure to the aqueous phase (especially under extreme pH conditions). This polishing was carried out using 1 μm and 1/4 μm diamond polishing compounds and Microcloth polishing cloths (Buehler). Polishing was always followed by H_2SO_4/NoChromix cleaning and copious water rinses to remove any surface active contaminants. Prior to all experimental runs, the cell was assembled and rinsed again with dilute $HClO_4$ followed by several rinses with H_2O. Chemicals were used without further purification and include: Sodium dodecyl sulfate (SigmaUltra, > 99% pure), $HClO_4$ (GFS Chemicals, 70% double distilled), NaOH (Aldrich, 99.998% pure), and D_2O (Cambridge Isotope Laboratories, 99.9%). All solutions were prepared using 18 MΩ water from a Nanopure filtration system. Solution pH was adjusted by small additions of $HClO_4$ and NaOH *via* micropipette. The solution pH was monitored with a glass combination electrode calibrated with pH 4, 7 and 10 standards. Equilibration of the system, following any additions made to the aqueous phase, was monitored by recording the signal intensity at the peak frequency of the water response over time (with stirring). Solutions typically reached steady-state after 15 min, but were allowed to equilibrate for 30 min before spectra were recorded. Equilibration times of up to 12 h were tested, but found to be unnecessary. Spectra were recorded, without stirring, at an increment of 2 cm^{-1}, with 40–80 pulses averaged per increment. Typically, five full spectra were recorded and averaged for each different solution composition.

Vibrational sum-frequency spectroscopy: Background and analysis

Vibrational sum-frequency spectroscopy (VSFS) is a surface specific, non-linear optical technique first predicted theoretically in 1962 by Bloembergen,[22] with experimental confirmation of that theory demonstrated by Shen in the late 1980's.[23,24] Experimentally, the VSFS response is generated by coupling two coherent, high intensity laser light sources spatially and temporally at an interface to generate a third beam at the sum of the two incident beam frequencies ($\omega_3 = \omega_1 + \omega_2$). Typically, these two beams include a fixed frequency visible beam and a tunable IR beam. The intensity of the incident light sources generates an oscillating nonlinear polarization of the molecules in the interfacial region which reradiates as the generated sum-frequency signal. Under the dipole approximation only molecules which experience a non-centrosymmetric environment will be sum-frequency active. Such an environment is created when two immiscible phases come into contact; thus, molecules which feel the effects of an interface will be sum-frequency active and can generate a VSFS response. The intensity of this response is governed by the square of the second order polarizability $P^{(2)}$ through following expression:

$$I_{SF} \propto \left|P^{(2)}\right|^2 \propto \left|\chi^{(2)}_{NR} e^{i\phi_{NR}} + \sum_{\nu} \chi^{(2)}_{R_\nu} e^{i\gamma_\nu}\right|^2 I_{Vis} I_{IR} \qquad (1)$$

where $P^{(2)}$ is the second order polarization of the medium, $\chi^{(2)}_{NR}$ and $\chi^{(2)}_{R_\nu}$ are the non-resonant and resonant responses of the surface nonlinear susceptibility, $e^{i\phi_{NR}}$ and $e^{i\gamma_\nu}$ are the phases of those responses, and I_{Vis} and I_{IR} are the intensities of the incident laser beams. The resonant contribution to the nonlinear susceptibility ($\chi^{(2)}_R$) can then be expressed as the following:

$$\left(\chi^{(2)}_{R_\nu}\right)_{IJK} \propto N \frac{A_K M_{IJ}}{\omega_\nu - \omega_{IR} - i\Gamma_\nu} \qquad (2)$$

where N is the number of responding molecules; A_K and M_{IJ} are the IR and Raman transition moments, respectively; ω_ν is the frequency of the vibrational resonance; ω_{IR} is the frequency of the incident IR beam; and Γ_ν is the natural linewidth of the transition. Therefore, for a vibration to be sum-frequency active it must possess both nonzero IR and Raman transition moments. Such is the case for modes which lack inversion symmetry. This fact, along with the non-centrosymmetric nature of the interface gives rise to the surface specificity of the sum-frequency response. The intensity of the response is resonantly enhanced by tuning the IR frequency ω_{IR} through a vibrational resonance, thus mapping out a spectrum of the interfacial molecules.

For these studies, the resonant modes examined occur in the mid-IR portion of the electromagnetic spectrum encompassing both the CH stretching region from ~2800–3000 cm^{-1}, as well as the OH stretching region from ~2800–3700 cm^{-1}. These different types of oscillators give rise to very different resonant spectral signatures for molecules in an aqueous environment. The CH modes are distinguished by narrow peaks, within a relatively narrow portion of the spectrum (~2800–3000 cm^{-1}). In contrast, the OH oscillators are strongly affected by the intermolecular hydrogen bonding environments that condensed phase water molecules experience. This leads to extensive spectral broadening as well as a shift in the band intensity as a function of the hydrogen bond strength.

As a result of the coherent nature of the sum-frequency process, the non-resonant component and each of the resonant components contained within the sum, has a unique phase associated with it as specified by the $e^{i\phi_{NR}}$ and $e^{i\gamma_\nu}$ terms in eqn. (1). The fact that the components for the nonlinear surface susceptibility $\chi^{(2)}_{R_\nu}$ and $\chi^{(2)}_{NR}$ are summed prior to squaring gives rise to constructive and destructive interferences between overlapping modes. While this tends to complicate the interpretation of the experimental data, it is also advantageous in that the interferences carry orientational information about

the molecules being probed. We take advantage of these interferences in order to further understand the relative orientation of the molecules in the interfacial region. This information comes from a spectral deconvolution and analysis routine developed in our laboratory and modeled after the procedure first introduced by Bain *et al.*[25] Spectral fits are based on the expression:

$$\chi_{\nu}^{(2)} = \int_{-\infty}^{\infty} \frac{A_{\nu}\exp\left(-[(\omega_L - \omega_{\nu})/\Gamma_{\nu}]^2\right)}{\omega - \omega_{\mathrm{L}} - \mathrm{i}\Gamma_{\mathrm{L}}}\,\mathrm{d}\omega_{\mathrm{L}} \qquad (2)$$

This expression for the resonant vibrational response convolves the homogeneous linewidth of the transition (Γ_{L}) with an expression to account for inhomogeneous broadening (Γ_{ν}) due to the multitude of environments that the molecules experience in the condensed phase. A_{ν} represents the effective sum-frequency transition strength which is proportional to the orientational averaged IR and Raman transition moments, and ω_{L} and ω_{ν} are the center frequencies of the Lorentzian and Gaussian bands, respectively. We make use of a series of tightly held constraints on the peak phases, widths and locations, obtained from spectra recorded in different environments, to attain curve fit parameters that are consistent across the different experimental systems.

Neat CaF_2/H_2O interface *vs.* pH

As a prelude to the upcoming surfactant studies, Fig. 1 shows the VSFS response from the CaF_2/H_2O interface as a function of pH.[18] A large variation in the spectral response from the interfacial water molecules is observed as the pH is altered.

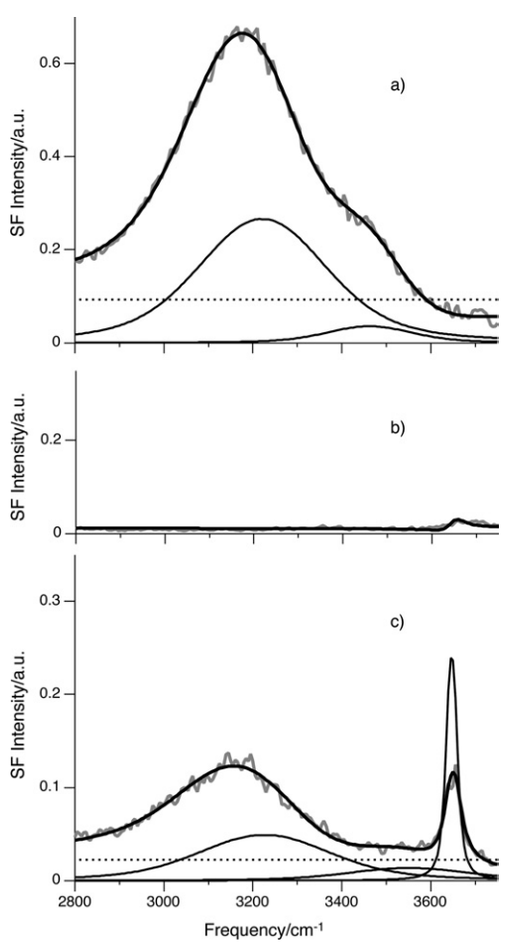

Fig. 1 VSFS spectra of the CaF_2/H_2O interface at pH (a) 2.9, (b) 6.4, and (c) 12.3. Experimental data is shown in grey. Curve fits and individual peak components are shown in black. The dotted line represents NR background signal.

At pH 2.9 (Fig. 1a), the spectrum shows a large VSFS response across the entire OH stretching region. The spectral fit obtained as described above is superimposed on the data along with the peaks contributing to that fit. The curve fitting parameters for the individual oscillator contributions are presented in Table 1. The data show a strong response centered at 3221 cm^{-1} from H_2O in a highly ordered, tetrahedrally coordinated environment and a smaller response at 3462 cm^{-1} from H_2O in a more disordered hydrogen bonding environment.[26,27] The water molecules contributing to this response are oriented, on average, with their oxygen atoms closest to the CaF_2 surface as determined from spectral fits from this data and the surfactant studies described later in this paper. We arbitrarily assign a phase of zero for this orientation.

The orientation and structuring of the interfacial water molecules is a result of the alignment of their molecular dipoles with the electric field present in the interfacial region. This field arises due to an excess of Ca^{2+} ions on the surface of the solid resulting from the preferential dissolution of surface F^- ions. Experiments studying the electrokinetic behavior of pulverized CaF_2 solid suspended in an acidic aqueous medium have measured the interfacial zeta potential at the plane of shear between the solid and aqueous phase to be in the range of 50–70 mV,[28–30] which translates into electric field strengths on the order of 10^6–10^7 V cm^{-1} near the surface of the solid. Field strengths of this magnitude can penetrate into the aqueous phase on the order of a nanometer or more.[2] At acidic pH's, like that shown in Fig. 1a, water molecules present near the surface of the CaF_2 solid experience a strong orientational force due to that electric field and orient themselves into a symmetric, tetrahedrally hydrogen bonded network. The behavior of the interfacial H_2O molecules near the CaF_2 surface parallels that of other solid/liquid systems studied previously.[27,31–34] It has been shown in all of these systems that the electric properties of the solid phase are the primary driving force for alignment and structuring of the H_2O molecules near the solid surface. The main difference between these prior studies and those detailed herein is the ionic, as compared to molecular, nature of the CaF_2 solid. The ionic and semi-soluble properties of the CaF_2 surface gives rise to a more chemically complex interfacial system whose surface composition is altered through adjustments in bulk pH and ion composition of the aqueous phase.

Increasing the pH of the solution results in a steady decrease of the VSFS signal from the interfacial H_2O molecules, until at pH 6.4 (Fig. 1b) the response is essentially zero except for a low intensity peak centered at 3647 cm^{-1} that becomes even more apparent at higher pH (see below). The lack of significant VSFS intensity in the OH stretch region at this pH is indicative of interfacial water molecules that are randomly oriented as the point of zero charge (p.z.c.) of the CaF_2/H_2O interface is approached. Several studies have determined the PZC of CaF_2 to be in the pH range of 5.4 to 7.8,[35–38] which agrees well with our experimental results.

The VSFS signal in the OH stretch region steadily increases as the pH is increased to 12.3. As the solution becomes more basic, the surface assumes an increasingly negative charge. It has been determined in previous studies, that CaF_2 in an aqueous environment undergoes an ion exchange reaction between the surface fluoride ions and hydroxide ions in solution.[4,39] This process, in conjunction with the dissociative adsorption of interfacial H_2O molecules, gives rise to the formation of the negatively charged surface. Bulk potentiometric titration experiments of the CaF_2/H_2O system indicate that this ion exchange reaction begins in the neutral pH range and dominates the interfacial chemistry at high pH (high OH^- concentration).[4] The spectral fit to the data in Fig. 1c is presented in Table 1 and includes three distinct contributions from interfacial water molecules. The first, centered at 3221 cm^{-1} is from the tetrahedrally coordinated water molecule

Table 1 Parameters determined from the nonlinear least-squares fits to the experimental data from the CaF_2/H_2O system at (a) pH 2.9 and (b) pH 12.3.

(a)

Oscillator	Amplitude[a]	Frequency/cm^{-1}	Width (Γ_L/cm^{-1})	Width (Γ_ν/cm^{-1})	Phase/rad
H_2O (ss)	0.53	3221 ± 5	5	169 ± 13	0.0 ± 0.1
H_2O (ss)	0.20	3462 ± 5	5	113 ± 8	0.0 ± 0.1

(b)

Oscillator	Amplitude[a]	Frequency/cm^{-1}	Width (Γ_L/cm^{-1})	Width (Γ_ν/cm^{-1})	Phase/rad
H_2O (ss)	0.23	3226 ± 5	5	173 ± 13	3.14 ± 0.1
H_2O (solvating)	0.12	3551 ± 5	5	160 ± 12	3.14 ± 0.1
Ca–OH	1.16	3647 ± 2	12	12 ± 1	0.0 ± 0.1

[a] In arbitrary units.

network discussed previously. We attribute the second feature centered at 3647 cm^{-1} to the CaOH species formed on the surface of the CaF_2 solid as a result of the surface ion exchange reaction.[18] The position and width of this feature indicates that these surface Ca–OH oscillators show only very weak hydrogen bond interactions with the overlying, tetrahedrally coordinated, water molecule network. A third peak, centered at 3551 cm^{-1} is also present, which we attribute to the weakly interacting water molecules with less than tetrahedral coordination situated directly above the CaOH surface. These weakly interacting water molecules have been detected in other studies by our group,[40,41] and typically involve solvating water molecules near charged ionic species. Orientational information provided by the curve fits indicate that the CaOH oscillators are oriented 180° out of phase from both the tetrahedral water molecule network and the weakly interacting solvating water molecules situated above the solid surface (see Table 1), giving strong evidence for our orientational interpretation. We note that the ion exchange reaction yielding the surface CaOH species is reversible, and adjusting the pH of the aqueous phase back into the neutral to acidic range removes these species from the surface resulting in a disappearance of the peak responses at 3647 cm^{-1} and 3551 cm^{-1}. In addition, previous studies on this system[18] show that increasing the concentration of F^- ions in solution will also drive the reaction towards reformation of the CaF_2 surface species at the expense of the $Ca(OH)_2$.

SDS adsorption at the CaF_2/H_2O and CaF_2/D_2O interfaces

Fig. 2 shows the spectra of the CaF_2/H_2O interface as a function of SDS concentration. This is a more extensive set of data than presented in our previous letter[19] which allows for a more complete picture of the SDS adsorption process. At pH 5.1 (Fig. 2a) the CaF_2 surface is positively charged and results in the alignment of interfacial water molecules into the highly coordinated network that was described in the previous section. Small additions of SDS to the solution (total SDS concentration = 2.0×10^{-5} to 1.2×10^{-4}) result in a significant decrease in the overall response from the interfacial water molecules across the entire OH stretching region as the interfacial charge is reduced upon surfactant adsorption (Fig. 2b–e). By 2×10^{-4} M (Fig. 2f), the surface charge is neutralized as evidenced by the negligible OH signal response. In addition, as surfactant molecules adsorb into the interfacial region they can displace the water molecules from that region resulting in a lowering of the VSFS response. There are also small but detectable responses from the CH oscillators of the surfactant over the range from 2850–2950 cm^{-1} that overlap and interfere destructively with the low energy tail of the water peak centered at ~3200 cm^{-1}. There is no observation of a "free OH" oscillator near 3700 cm^{-1} as has been seen at other aqueous interfaces[31,42–44] indicating no strong orientation of water molecules with one OH bound to the salt surface and the other to the surrounding water molecules.

The implied electrical properties of this system parallel those found in experiments studying surfactant adsorption onto charge-regulated substrates by Bard and coworkers.[45] These studies used atomic force microscopy (AFM) measurements to follow the adsorption of negatively charged SDS molecules onto a well defined, positively charged surface at the terminus of a self-assembled monolayer. The conclusion from these experiments is that charge neutralization, as a result of adsorption between an oppositely charged substrate and a surfactant

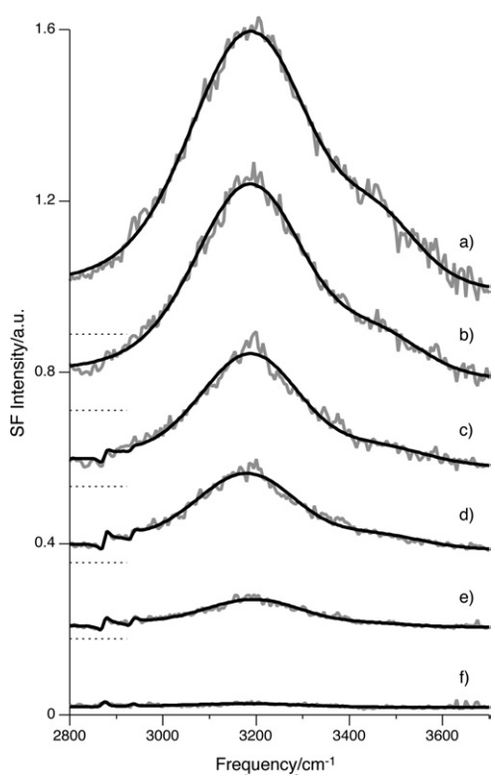

Fig. 2 VSFS spectra of the positively charged $CaF_2/H_2O/SDS$ interface at pH 5.1 and SDS concentrations of (a) neat CaF_2/H_2O, (b) 2.0×10^{-5} M, (c) 5.0×10^{-5} M, (d) 6.1×10^{-5} M, (e) 1.2×10^{-4} M, and (f) 2.0×10^{-4} M. Spectra are offset for clarity, with the zero signal level for a–e shown as a dotted line.

can occur at surfactant concentrations well below the critical micelle concentration (c.m.c.) of the adsorbing species. Such is the case in our experiments, where the concentration of SDS is approximately 1/40th of the c.m.c. of sodium dodecylsulfate.

At higher SDS concentrations the spectral response across the entire OH stretching region increases as a function of increasing SDS concentration. The increased signal at ~3200 cm^{-1} and ~3450 cm^{-1} observed in Fig. 3 indicates that at higher SDS concentrations, water molecules are again oriented as a result of the electric field present at the interface. The spectra show constructive interferences between the CH oscillators comprising the surfactant tail and the broad response from the OH oscillators of the interfacial water molecules. The change in the qualitative shape of the CH modes present in Figs. 2 and 3 is the result of the change from destructive to constructive interferences between the OH and CH modes due to a reorientation of water molecules. These interferences will be more quantitatively addressed later in the paper, when spectral fitting procedures are applied to the surfactant data.

In order to simplify the spectra and obtain quantitative information about the contributing CH and OH modes, we conducted a series of CaF_2/D_2O/SDS experiments analogous to the previously detailed CaF_2/H_2O/SDS data. The VSFS response from interfacial OD oscillators are shifted down in energy by ~1000 cm^{-1} from their OH counterparts[26] effectively removing their influence from the 2800–3000 cm^{-1} region where the CH modes reside. Spectral fitting routines were applied to both sets of data simultaneously for a detailed determination of the peak parameters (*e.g.* peak locations, peak widths and relative phases between modes). This allows orientational information about the molecules in the interfacial region to be obtained over the range of surfactant concentrations studied. For a typical set of experiments, we fit the data for both systems (H_2O and D_2O at equivalent SDS concentrations) holding the CH peak parameters constant and maximizing fit accuracy between the data sets by iterating between the two different systems. The results are fits which hold true for both types of data sets, with the difference being the inclusion of peaks due to the OH oscillators in the CaF_2/H_2O/SDS system.

Fig. 4 shows a series of spectra for varying concentrations of SDS in D_2O that can be compared with Figs. 2 and 3. Fig. 4a shows the featureless, but non-zero, non-resonant spectrum of the neat CaF_2/D_2O interface. With low concentrations of SDS (1×10^{-4} M SDS) in the aqueous phase (Fig. 4b), two small features from the CH oscillators are evident and determined by the spectral fits (see below) to reside at 2873 cm^{-1} and 2934 cm^{-1}. These responses correspond to the symmetric stretch of the terminal CH_3 split by a Fermi resonance with an overtone of the CH_3 bending mode.[43,46–48] As later spectra show, the oscillator strength for the CH stretches is quite strong; therefore, the lack of significant response indicates that those molecules which have adsorbed to the surface are considerably disordered, resulting in a nearly isotropic layer of surfactant molecules with only a minor degree of orientation of the terminal CH_3 groups. Because of their more random, isotropic distribution we only see a minor sum-frequency response from these CH_3 oscillators. In contrast, surfactants which adsorb in very ordered monolayers (sodium oleate, sodium stearate) on CaF_2 give rise to considerably larger CH responses compared to the CaF_2/SDS systems.[49]

At higher concentrations (5×10^{-4} M SDS) the contribution from the terminal CH_3 oscillators (2873 cm^{-1} and 2934 cm^{-1}) has increased by ~250% relative to the 1×10^{-4} M SDS concentration (Fig. 4c). The increased response of the CH_3 groups indicates not only that there are a larger number of these oscillators in the interfacial region, but also that the terminal groups are now oriented perpendicular to the interfacial plane to a larger extent. Further evidence for the perpendicular orientation of these oscillators comes from SPS spectra

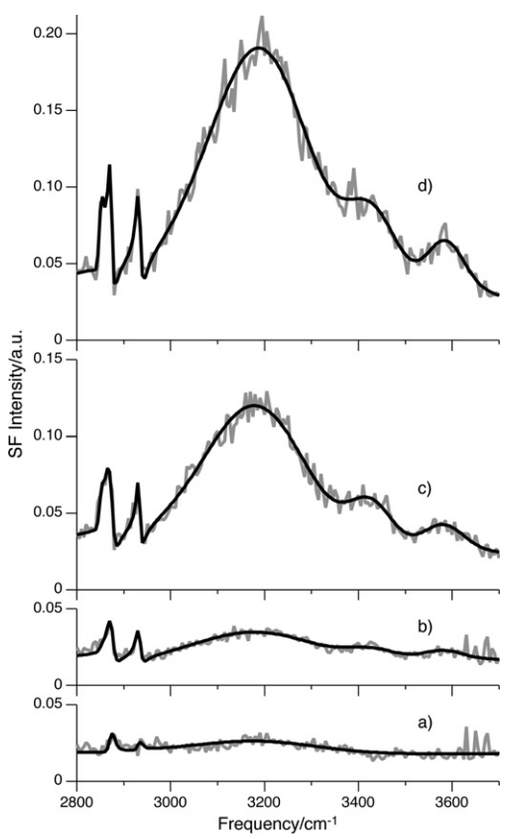

Fig. 3 VSFS spectra of the negatively charged CaF_2/H_2O/SDS interface at pH 5.1 and SDS concentrations of (a) 2.0×10^{-4} M, (b) 3.5×10^{-4} M, (c) 5.6×10^{-4} M, and (d) 9.2×10^{-4} M.

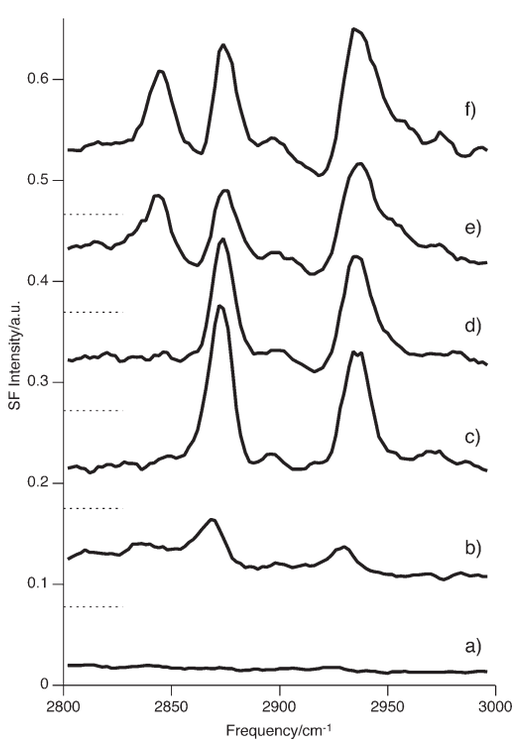

Fig. 4 VSFS spectra of CaF_2/D_2O/SDS interface in the CH stretching region at SDS concentrations of (a) neat CaF_2/D_2O, (b) 1.0×10^{-4} M, (c) 5.0×10^{-4} M, (d) 1.0×10^{-3} M, (e) 5.0×10^{-3} M, and (f) 9×10^{-3} M. Spectra are offset for clarity, with the zero signal level for b–f shown as a dotted line.

presented later in this section. Continued increases in SDS surfactant concentration results in a reversal in the intensity trend. As shown in Fig. 4d and determined from the spectral fits, increased surfactant adsorption results in a slight decrease (~20% lower) in CH_3 oscillators at 2873 cm^{-1} even though the concentration of the surfactant in solution has doubled to 1×10^{-3} M. The overall decrease in the response from the CH_3 oscillators as a function of increasing SDS concentration continues as the solution concentration is increased to 5×10^{-3} M (Fig. 4e). Given that adsorption of the surfactant molecules continues to occur in this concentration region, as manifested in changes in the OH band intensities, this lack of significant increase in intensity from the methyl oscillators must be due to either bilayer formation or additional monomers forcing significant disordering of the monolayer. This will be discussed in more detail in a later section. Disordering is clearly apparent in this concentration regime as a new peak appears in the spectrum at 2849 cm^{-1} that we assign to the symmetric stretch of methylene groups along the surfactant tail backbone. These CH_2 oscillators begin to appear as a result of *gauche* defects in the surfactant tails, which remove the local inversion symmetry found in an all trans configuration. The methylene modes increasingly contribute to the spectra as a function of added surface concentration (Fig. 4e–f), indicating that additional surfactant molecules adsorbing at the surface have more *gauche* defects than their earlier counterparts, or that additional surfactant adsorption causes an increase in *gauche* defects in all the adsorbed surfactants. A small increase in the CH_3 signal is observed at the highest concentration, however it should be noted that the system is now above the critical micelle concentration (c.m.c.) for SDS in water (c.m.c. $\approx 8 \times 10^{-3}$ M)[50] and above the solubility limit of solid calcium dodecylsulfate[38] complicating further interpretation of the trends seen previously.

Further insight into the behavior of the surfactant chains can be obtained by examining the system under different polarization schemes. Fig. 5 shows the SPS polarization spectra of the CaF_2/D_2O/SDS interface at the neat CaF_2/D_2O interface and at a range of SDS concentrations from 0 to 5×10^{-2} M. The SPS polarization scheme probes dipole transition moments with components parallel to the interfacial plane. The neat CaF_2/D_2O interface is shown in Fig. 5a with a featureless, but non-zero non-resonant background. Increasing the bulk SDS concentration from 0 to 5×10^{-2} M results in the spectra shown in Fig. 5b–e. There is a single peak response from a vibrational mode at 2956 cm^{-1} which we assign to the asymmetric stretch of the CH_3 group at the terminus of the surfactant chain.[43,46–48] The spectra show only minor decreases in the CH_3(as) as the SDS concentration is increased with no other discernable features appearing in the spectra across all of the SDS concentrations examined.

Fig. 6 compares the data, spectral fits and spectral components for SDS (3×10^{-3} M) at the CaF_2/D_2O (Fig. 6b) and CaF_2/H_2O (Fig. 6a) interfaces. As noted above, the fit to the data shown in Fig. 6 is achieved by constraining the CH peak parameters to be strictly equal in both Figs. 6a and 6b and then including a contribution from the OH oscillators in the CaF_2/H_2O/SDS system. The result is excellent fit across both sets of data using these restrictive spectral constraints. A cursory examination of the figures points out the qualitative differences in the spectra between the two physically similar systems. The 3×10^{-3} M SDS in D_2O spectrum (Fig. 6b) shows minimal (but evident) interferences between the contributing CH modes and the non-resonant background; however, the closely spaced modes are still well resolved. In comparison, the H_2O spectrum shows interferences between each individual CH mode, as well as strong constructive and destructive interferences with the slowly decreasing "tail" of the OH vibrational response from 3000–2800 cm^{-1} (from the peak centered at 3221 cm^{-1}). For the SDS/CaF_2/D_2O data an excellent

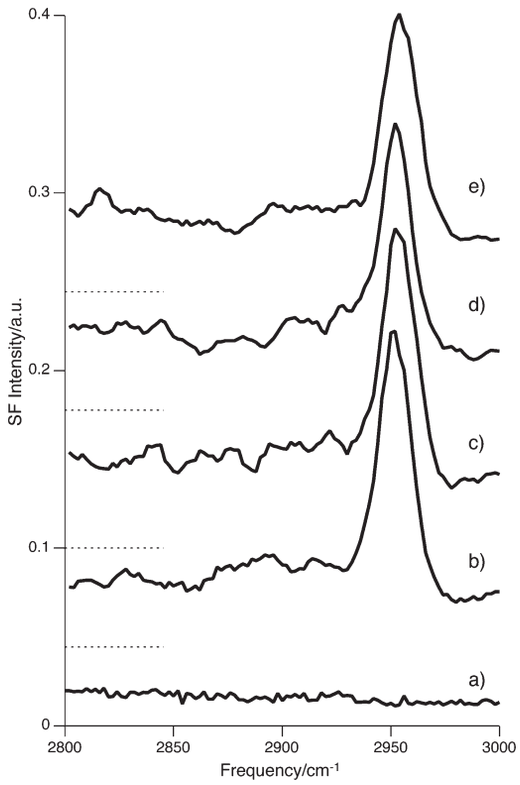

Fig. 5 VSFS spectra (SPS polarization) of CaF_2/D_2O/SDS interface at SDS concentrations of (a) neat CaF_2/D_2O, (b) 5.0×10^{-4} M, (c) 1.0×10^{-3} M, (d) 5.0×10^{-3} M, and (e) 1.0×10^{-2} M. Spectra are offset for clarity, with the zero signal level for b–e shown as a dotted line.

fit is obtained by including contributions from four resonant CH vibrations and the non-resonant background. Two features are assigned to the symmetric stretch of methylene CH_2 groups split by a Fermi resonance with the overtone of its

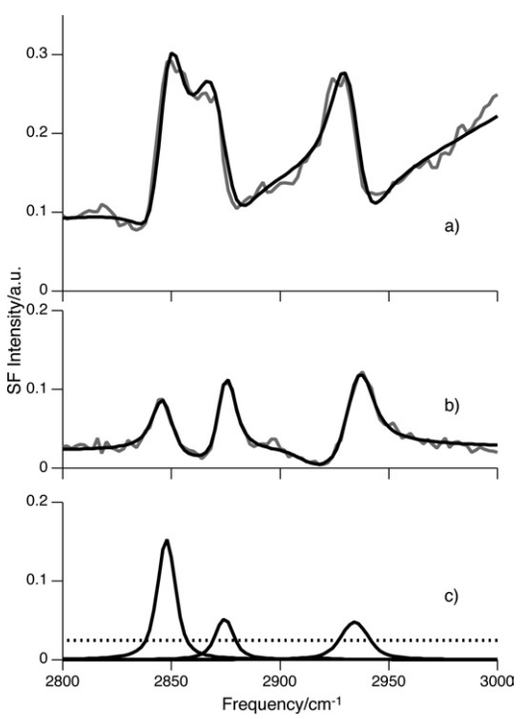

Fig. 6 VSFS spectra and curve fits for 3.0×10^{-3} M SDS in (a) H_2O and (b) D_2O, along with (c) the resulting component peaks (and NR background (dashed)) from those curve fits. Note the alteration in shape and apparent shift in peak intensity and location due to the interferences between contributing modes.

deformation mode (2849 cm^{-1} and 2905 cm^{-1}).[48,51,52] The second two features are assigned to a CH_3 symmetric stretch also split by a Fermi resonance with an overtone of its deformation mode (2873 cm^{-1} and 2934 cm^{-1}).[48,51,52] The peak parameters for this fit are included in Table 2. The phases of the contributing modes are constrained by symmetry to be the same (held within ± 0.1 radian) with their corresponding Fermi resonances. The phase relationship between the CH_2 and CH_3 modes is unknown, and therefore was allowed to adjust in order to best fit the data. Generally, this relative phase difference was found to be close to $\pi/2$ in all of our fits.

Fig. 7 shows experimental data from the CaF_2/H_2O system at 9×10^{-3} M SDS along with the curve fit to the data and each of the individual oscillator contributions. As the figure shows, we can achieve a very good fit to the experimental data across the entire CH and OH stretching regions. This particular curve fit is comprised of all of the peak responses discussed previously including four contributions from the CH_2 and CH_3 oscillators and two contributions from the symmetrically bound and asymmetrically bound H_2O molecules. The H_2O spectra also contain an additional broad peak centered at 3567 cm^{-1} that we attribute to water molecules solvating the negatively charged sulfate headgroup of the SDS. A broad peak in this region has also been observed in previous VSFS studies of ions at the CCl_4/H_2O interface.[41,53] In these previous studies this peak, in the weakly hydrogen bonded water region, was also attributed to water molecules solvating the sulfate headgroup of adsorbed SDS. It is interesting to note in Fig. 7, the strong influence that the tailing wings of the broad OH oscillator response have on the overall spectra. The most intense peak from the tetrahedrally bound H_2O molecules at $\sim$3200 cm^{-1}, influences and interferes with all of the other peak contributions across the entire region; which illustrates well, the need for the D_2O studies to remove these interferences to better characterize the individual peak contributions. The parameters used in all these fits are included in Table 2.

Water orientation upon surfactant adsorption

In our earlier letter[19] we describe the charge reversal phenomena observed in the CaF_2/H_2O/SDS system based on a simple inspection of the data. As noted in this publication, charge reversal on the CaF_2 surface should manifest itself in a 180° flip in the orientation of the interfacial water molecules, with a corresponding change in the spectral interferences between the OH and CH modes. This observed change in the spectral features was suggestive of such a water reorientation but further experiments and spectral fitting were deemed necessary for confirmation.

Table 3 is a compilation of the spectral parameters for the CaF_2/H_2O/SDS system under conditions where the surface is positively charged (4.1×10^{-5} M SDS; Table 3a) and negatively charged (9.1×10^{-4} M SDS; Table 3b), as determined from the combined fitting of the H_2O and D_2O spectra. When the surface is positively charged (Table 3a; Fig. 2) the spectra

Table 2 Parameters determined from the nonlinear least-squares fits to the experimental data from the CaF_2/H_2O/SDS and CaF_2/D_2O/SDS systems at 3.0×10^{-3} M SDS.

Oscillator	Frequency/ cm^{-1}	Width (Γ_L/cm^{-1})	Width (Γ_ν/cm^{-1})	Phase/ rad
CH_2 (ss)	2849 ± 1	2	5 ± 1	1.6 ± 0.1
CH_2 (ss-FR)	2905 ± 1	2	8 ± 1	1.6 ± 0.1
CH_3 (ss)	2873 ± 1	2	5 ± 1	0.0 ± 0.1
CH_3 (ss-FR)	2934 ± 1	2	6 ± 1	0.0 ± 0.1
H_2O (ss)	3218 ± 5	5	170 ± 15	0.0 ± 0.2
H_2O (ss)	3418 ± 5	5	61 ± 5	0.0 ± 0.2
H_2O (solvating)	3567 ± 5	5	52 ± 5	0.0 ± 0.2

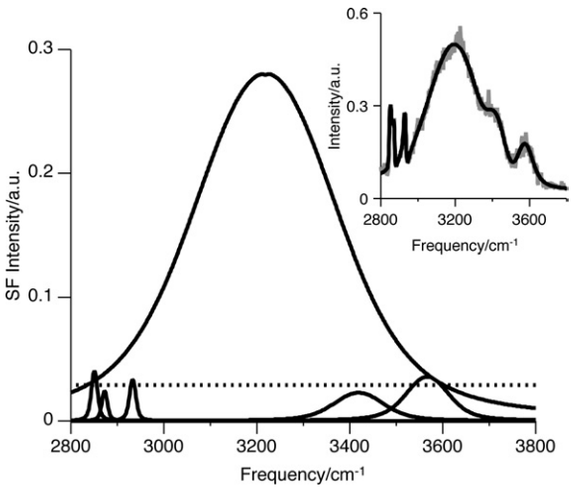

Fig. 7 The peak components from the curve fit to the CaF_2/H_2O/SDS interface at 9×10^{-3} M SDS (the spectral data and curve fit are included as an inset), spanning the entire CH and OH stretching regions.

show a strong response from interfacial water molecules at 3218 cm^{-1} that "tails off" across the CH stretching region and interferes destructively with the CH responses from the small number of adsorbed SDS molecules. In our curve fits we assign a phase of zero (arbitrarily) to the CH_3(ss) mode from the adsorbed SDS molecules and fit the remaining peaks relative to that value. From the spectral fits at this concentration, a phase difference of 180° is found for the OH(ss) mode relative to the CH_3(ss) mode. This is consistent with the picture that the water molecules are oriented, on average, with their oxygen atoms nearest to the CaF_2 surface. At higher surfactant concentrations (as shown in Fig. 3) the system has passed through the point of surface charge neutralization. The corresponding reversal of the surface charge manifests itself in a change from constructive to destructive interferences between the contributing CH and OH vibrational modes. The data in Table 3 reflects this reorientation of the interfacial H_2O molecules through a 180° phase change from the contributing OH oscillators as compared to the contributing CH_3(ss) modes. The water molecules are now oriented, on average, with their oxygen atoms furthest away from the CaF_2 surface and their hydrogen atoms pointing toward the surface. In fitting the experimental data, we have constrained the peak positions, widths and phases of all of the contributing CH modes due to the adsorbed SDS molecules and allowed for the 180° phase change in the VSFS response as a result of the reorientation of the OH oscillators. Additionally, it is necessary to also adjust the phase of the non-resonant background response by 180°. This change in phase is expected because both the non-resonant and resonant contributions to the molecular hyperpolarizability, contained in the expression for χ, are generated by the molecules in the interfacial region. As those molecules flip their orientation, the response from both the resonant and non-resonant components of that hyperpolarizability are expected to exhibit similar changes in relative phase behavior. We are able to achieve very good fits across all of our data sets with the tight constraints imposed and the inclusion of the 180° phase flip of the OH oscillators due to the reorientation of the water molecules in the interfacial region, thus giving strong evidence for our orientational interpretation.

Surfactant assembly and conformation

It is clear from the above discussion that the adsorption of surfactant at the CaF_2/aqueous interface initially neutralizes the positive surface charge of the CaF_2 solid to the point at which the net electric field is zero. With continued buildup of

Table 3 Parameters determined from the nonlinear least-squares fits to the experimental data from the $CaF_2/H_2O/SDS$ system at (a) 4.1×10^{-5} M SDS, prior to charge reversal; and at (b) 9.1×10^{-4} M SDS, past charge reversal.

(a)

Oscillator	Amplitude[a]	Frequency/cm^{-1}	Width (Γ_L/cm^{-1})	Width (Γ_ν/cm^{-1})	Phase/rad
CH_2 (ss)	0.02	2851 ± 1	2	7 ± 1	1.67 ± 0.1
CH_3 (ss)	0.10	2873 ± 1	2	6 ± 1	0.0 ± 0.1
CH_3 (ss-FR)	0.07	2932 ± 1	2	6 ± 1	0.0 ± 0.1
H_2O (ss)	0.39	3218 ± 5	5	170 ± 13	3.14 ± 0.1

(b)

Oscillator	Amplitude[a]	Frequency/cm^{-1}	Width (Γ_L/cm^{-1})	Width (Γ_ν/cm^{-1})	Phase/rad
CH_2 (ss)	0.11	2851 ± 1	2	6 ± 1	1.76 ± 0.1
CH_3 (ss)	0.21	2873 ± 1	2	5 ± 1	0.0 ± 0.1
CH_3 (ss-FR)	0.17	2933 ± 1	2	7 ± 1	0.0 ± 0.1
H_2O (ss)	0.42	3218 ± 5	5	161 ± 12	0.0 ± 0.1

[a] In arbitrary units.

surfactant, the surface becomes increasingly negative. This excess build up of surfactant must be due to either continued monolayer formation and/or the formation of a bilayer of SDS on the CaF_2 surface. Given the relatively rough nature of the CaF_2 surface in an aqueous solution, any bilayer formation would not fit the idealized picture of a bilayer of significant lateral regularity. A roughened bilayer structure, such as this, has been put forth by Quist *et al.*,[54] as one possible geometry for SDS molecules adsorbing onto similarly charged α-Al_2O_3 substrates.

In our studies, the $CaF_2/D_2O/SDS$ data provide insight into this issue. Beyond a solution concentration of 5×10^{-4} M, increased surfactant adsorption results in a slight decrease in the CH_3 oscillator response at 2873 cm^{-1}, even as the concentration of the surfactant in solution has increased by a factor of 10. In addition, continued adsorption of SDS molecules to the surface is accompanied by an increase in chain disorder resulting in the appearance of the CH_2(ss) mode at 2850 cm^{-1}. The decrease in peak response gives support for the initiation of a bilayer of SDS molecules forming on portions of the CaF_2 surface. As the SDS molecules begin to adsorb into the bilayer, their hydrophobic tails will be oriented, on average, in the opposite direction from the monolayer already adsorbed on the surface. This results in an overall cancellation of the sum-frequency response from the CH_3 vibrations due to their opposite phases (with the formation of the bilayer the system has become more centrosymmetric) and a corresponding decrease in the VSFS response.

We conducted a thorough fitting analysis of the data to examine if such a bilayer formation was supported by fits to the data. It is important to note that in order to minimize the number of adjustable parameters required to obtain a good fit and still attain physically meaningful results we constrained the phase of the CH modes across all of the curve fits. If we remove this constraint the data can be fit equally well (and in some cases better) than those fits without constraints. In the case where phase is used as an adjustable parameter, we observe a change in phase of 1.8 radians as the concentration of SDS is increased from 1×10^{-4} M to 5×10^{-3} M. This observed phase change is consistent with the type of interference that would be expected as chains of opposite orientation begin to form the bilayer structure. In either case, holding the phase constant or allowing it as an adjustable parameter, the intensity of the CH_3 response steadily decreases between 5×10^{-4} M and 5×10^{-3} M SDS as a result of the initiation of bilayer formation.

Further support for bilayer formation comes from combining the results from both the $CaF_2/H_2O/SDS$ and $CaF_2/D_2O/SDS$ systems. The $CaF_2/H_2O/SDS$ experiments show clear evidence for a charge reversal just below this concentration range as seen in the increase in response from the highly coordinated water at $\sim$3200 cm^{-1} and the 180° phase flip in the curve fits to this data. In the $CaF_2/H_2O/SDS$ system, increases in SDS concentration from 3.5×10^{-4} M to 9.2×10^{-4} M SDS (Figs. 3b–d) give rise to a marked increase in sum-frequency intensity from interfacial water molecules, indicating that an increase in the number of surfactant molecules adsorbed on the CaF_2 surface are orienting these water molecules. However, in the $CaF_2/D_2O/SDS$ system this increase in adsorbed SDS molecules leads to a decrease in the CH_3 response. If the SDS molecules continued to primarily adsorb as a more densely packed monolayer in the interfacial region, one would expect an increase in the response from the terminal CH oscillators, which is not supported by our experimental data. Our results, however do not preclude the possibility that at SDS concentrations between 3.5×10^{-4} and 1×10^{-3} M there is a combination of both types adsorption (monomer and bilayer) occurring in the two systems studied. Bulk adsorption studies[10] suggest that bilayer formation occurs in the CaF_2/SDS system at above 1×10^{-3} M SDS, a concentration where we begin to see large changes in our spectra from the $CaF_2/D_2O/SDS$ system. These results, in conjunction with our spectra indicate that at intermediate SDS concentrations (between 3.5×10^{-4} M and 1×10^{-3} M) there may be a combination of monomer adsorption as well as and bilayer formation; whereas at concentrations above 1×10^{-3} M SDS bilayer formation begins to dominate the adsorption process. This manifests itself in a detectable decrease in the response from the CH_3 oscillators and the appearance of the CH_2 oscillators at these higher concentrations. Energetically, bilayer formation, with the surfactant molecules associating through Van der Waals interactions between their disordered tails, is favorable as compared to continued monomer adsorption. This is due to both a decrease in the charge repulsion between the sulfate headgroups on the surface and minimization of the exposure of the hydrophobic surfactant tails to the aqueous phase. In addition, the orientation of the surfactant molecules towards the aqueous phase allows for solvation of the headgroups (as is observed in a peak response at 3567 cm^{-1} in the $CaF_2/H_2O/SDS$ experiments) which also reduces the total energy of the system.[55]

Conclusions

We have presented studies of SDS adsorption at the CaF_2/D_2O interface that allows a more complete understanding of

surfactant adsorption at the CaF_2/H_2O interface. These studies, coupled with a more extensive analysis of the data reported in our previous letters, provides a comprehensive understanding of the dramatic changes in the structure and orientation of interfacial water molecules near the ionic solid, CaF_2, as a function of aqueous phase composition. Utilizing vibrational sum-frequency spectroscopy we examine the changes in the interfacial water structure and orientation as a function of pH, ion composition, and surfactant adsorption. We make use of experiments conducted in H_2O, in conjunction with a series of new experiments conducted in D_2O, in order to study how surfactant adsorption affects interfacial water molecules as well as the hydrophobic surfactant tails. The coherent nature of the VSFS response leads to spectral features which contain orientational information about the molecules at the interface. The D_2O studies reported help to remove ambiguities in the spectral interpretation due to the interferences between overlapping vibrational modes and enable an understanding of the interfacial behavior over a broad range of surfactant concentration. Detailed spectral analyses confirm the orientational changes which occur as a result of the changes in the electrical properties of the surface.

We have shown that the ionic nature and semi solubility of the CaF_2 solid lead to variations in the electrical properties of the surface as a function of the pH of the aqueous phase. In an acidic media, the positively charged CaF_2 surface aligns water molecules into a tetrahedrally coordinated network resulting in a strong sum-frequency response from these molecules. At neutral pH, the surface charge on the CaF_2 solid is greatly diminished, resulting in randomization of the water molecules and a total loss of sum-frequency signal. At high pH, the surface of the CaF_2 solid reverses charge and again orients the interfacial water molecules. In addition, an ion exchange reaction between surface fluoride ions and hydroxide ions in solution leads to the formation of CaOH on the surface of the solid.

We have also shown that the water molecule structure at the positively charged CaF_2 surface is greatly affected by adsorption of the oppositely charged SDS surfactant. Our studies indicate that as the SDS adsorbs to the surface, the surface charge steadily diminishes until at $\sim 2 \times 10^{-4}$ M SDS the charge is neutralized. This adsorption behavior results in a complete randomization of the water molecules above that surface and a commensurate loss in sum-frequency signal from those molecules. Further increases in concentration lead to the initiation of bilayer formation on at least portions of the CaF_2 surface which reorients the water molecules as shown in the $CaF_2/H_2O/SDS$ system. This bilayer initiation does not preclude the possibility of continued monomer adsorption to the interface. However, bilayer formation is energetically favorable and is suggested in the D_2O studies by a steady decrease in the CH_3 response as a function of increasing surfactant concentration. In addition, the bilayer structure orients the surfactant headgroups towards the aqueous phase, which results in a 180° flip in the water molecule orientation and solvation of the surfactant headgroups. We are able to confirm this orientational flip in the interfacial water molecules by carrying out a series of tightly constrained curve fits to our experimental data.

The information provided by fundamental experiments such as these, are important to further our understanding of the interactions between a sparingly soluble ionic solid, such as CaF_2, and an aqueous phase. The dynamic nature of these interfaces leads to large variations in the surface charge, water structure, and water molecule orientation as a function of pH, surfactant ion concentration, and ion composition of the aqueous phase. Information provided by these studies is essential for understanding such industrially relevant processes as mineral ore flotation, waste processing, and petroleum recovery.

Acknowledgements

The authors gratefully acknowledge Dr Mehmet Hancer and Dr Jan Miller at the University of Utah for their helpful assistance with the initial experiments and for continued interest and ongoing discussions. The authors also acknowledge the financial support of the Department of Energy, Basic Energy Sciences DE-FG06-96ER45273 and the Petroleum Research Fund of the American Chemical Society. One author (F.M.) acknowledges the sabbatical support provided by Whitman College.

References

1 H. S. Hanna and P. Somasundaran, in *Flotation of Salt-Type Minerals*, ed. M. C. Fuerstenau, American Institute of Mining, Metallurgical, and Petroleum Engineers, Inc., New York, 1976.
2 A. W. Adamson, *Physical Chemistry of Surfaces*, John Wiley & Sons, Inc., New York, 1990.
3 D. Myers, *Surfaces, Interfaces, and Colloids. Principles and Applications*, John Wiley & Sons, New York, 1999.
4 L. Wu and W. Forsling, *J. Colloid Interface Sci.*, 1995, **174**, 178–184.
5 Y. Hu, Y. Lu, S. Veeramasuneni and J. D. Miller, *J. Colloid Interface Sci.*, 1997, **190**, 224–231.
6 A. Holmgren, L. Wu and W. Forsling, *Spectrochim. Acta, Part A*, 1994, **50A**, 1857–1869.
7 P. B. Barraclough and P. G. Hall, *J. Chem. Soc., Faraday Trans.*, 1975, **71**, 2266–2276.
8 Y. Kuroda, *J. Chem. Soc., Faraday Trans.*, 1985, **81**, 757–768.
9 Y. Kuroda, H. Sato and T. Morimoto, *J. Colloid Interface Sci.*, 1985, **108**, 341–346.
10 M. L. Gonzalez-Martin and C. H. Rochester, *J. Chem. Soc., Faraday Trans.*, 1992, **88**, 873–878.
11 B. Popping, A. Deratani, B. Sebille, N. Desbois, J. M. Lamarche and A. Foissy, *Colloids Surf.*, 1992, **64**, 125–133.
12 J. Drelich, A. A. Atia, M. R. Yalamanchili and J. D. Miller, *J. Colloid Interface Sci.*, 1996, **178**, 720–732.
13 J. Drelich, W.-H. Jang and J. D. Miller, *Langmuir*, 1997, **13**, 1345–1351.
14 B. Janczuk, M. L. Gonzalez-Martin and J. M. Bruque, *Appl. Surf. Sci.*, 1994, **81**, 95–102.
15 E. Mielczarski, P. de Donato, J. A. Mielczarski, J. M. Cases, O. Barres and E. Bouquet, *J. Colloid Interface Sci.*, 2000, **226**, 269–276.
16 E. Mielczarski, J. A. Mielczarski and J. M. Cases, *Langmuir*, 1998, **14**, 1739–1747.
17 F. G. Moore, K. A. Becraft and G. L. Richmond, *Appl. Spectrosc.*, 2002, **56**, 1575–1578.
18 K. A. Becraft and G. L. Richmond, *Langmuir*, 2001, **17**, 7721–7724.
19 K. A. Becraft, F. G. Moore and G. L. Richmond, *J. Phys. Chem. B*, 2003, **107**, 3675–3678.
20 L. F. Scatena and G. L. Richmond, *J. Phys. Chem. B*, 2001, **105**, 11 240–11 250.
21 J. Löbau and K. Wolfrum, *J. Opt. Soc. Am. B*, 1997, **14**, 2505–2512.
22 N. Bloembergen and P. S. Pershan, *Phys. Rev.*, 1962, **128**, 606–622.
23 X. D. Zhu, H. Suhr and Y. R. Shen, *Phys. Rev. B: Condens. Matter*, 1987, **35**, 3047–3050.
24 P. Guyot-Sionnest, J. H. Hunt and Y. R. Shen, *Phys. Rev. Lett.*, 1987, **59**, 1597–1600.
25 C. D. Bain, P. B. Davies, T. H. Ong and R. N. Ward, *Langmuir*, 1991, **7**, 1563–1566.
26 J. R. Scherer, in *The Vibrational Spectroscopy of Water*, eds. R. J. H. Clark and R. E. Hester, London, 1978.
27 Q. Du, E. Freysz and Y. R. Shen, *Phys. Rev. Lett.*, 1994, **72**, 238–241.
28 K. H. Rao, J. M. Cases and K. S. E. Forssberg, *J. Colloid Interface Sci.*, 1991, **145**, 330–348.
29 L. Wu, W. Forsling and A. Holmgren, *J. Colloid Interface Sci.*, 2000, **224**, 211–218.
30 J. D. Miller and J. B. Hiskey, *J. Colloid Interface Sci.*, 1972, **41**, 567–573.
31 Q. Du, E. Freysz and Y. R. Shen, *Science*, 1994, **264**, 826–828.
32 S. Ye, S. Nihonyanagi and K. Uosaki, *Chemistry Letters*, 2000, **7**, 734–735.

33 J. Kim, G. Kim and P. S. Cremer, *Langmuir*, 2001, **17**, 7255–7260.
34 P. B. Miranda and Y. R. Shen, *J. Phys. Chem. B*, 1999, **103**, 3292–3307.
35 H. S. Choi, *Can. Metallurg. Q.*, 1963, **2**, 410–414.
36 M. S. Smani,B. P. and J. M. Cases, *Transactions of the American Institute of Mining and Metallurgical Engineers*, 1975, **258**, 168–173.
37 J. C. Le Bell and L. Lindstrom, *Finn. Chem. Lett.*, 1982, 134–138.
38 J. Oberndorfer and B. Dobias, *Colloids Surf.*, 1989, **41**, 69–76.
39 Y. Wu, J. T. Mayer, E. Garfunkel and T. E. Madey, *Langmuir*, 1994, **10**, 1482–1487.
40 E. A. Raymond and G. L. Richmond, *J. Phys. Chem. B*, in press.
41 L. F. Scatena and G. L. Richmond, *Chem. Phys. Lett.*, 2004, **383**, 491–495.
42 G. L. Richmond, *Chem. Rev.*, 2002, **102**, 2693–2724.
43 S. Ye, S. Nihonyanagi and K. Uosaki, *Phys. Chem. Chem. Phys.*, 2001, **3**, 3463–3469.
44 D. S. Walker, M. G. Brown, C. L. McFearin and G. L. Richmond, *J. Phys. Chem. B*, 2004, **108**, 2111–2114.
45 K. Hu and A. J. Bard, *Langmuir*, 1997, **13**, 5418–5425.
46 M. R. Watry and G. L. Richmond, *Langmuir*, 2002, **18**, 8881–8887.
47 S. R. Goates, D. A. Schofield and C. D. Bain, *Langmuir*, 1999, **15**, 1400–1409.
48 Y. Liu, L. K. Wolf and M. C. Messmer, *Langmuir*, 2001, **17**, 4329–4335.
49 K. A. Becraft and G. L. Richmond, in preparation.
50 D. Myers, *Surfactant Science and Technology*, VCH Publishers, Inc., New York, 1992.
51 R. N. Ward, D. C. Duffy, P. B. Davies and C. D. Bain, *J. Phys. Chem.*, 1994, **98**, 8536–8542.
52 R. G. Snyder, S. L. Hsu and S. Krimm, *Spectrochim. Acta, Part A*, 1978, **34A**, 395–406.
53 L. F. Scatena, *Vibrational Sum Frequency Spectroscopic Investigations of the Structure, Hydrogen Bonding, and Orientation of Water Molecules at the Liquid/Liquid Interface*, University of Oregon, Eugene, OR, 2002.
54 P.-O. Quist and E. Söderlind, *J. Colloid Interface Sci.*, 1995, **172**, 510–517.
55 J. F. Scamehorn, R. S. Schechter and W. H. Wade, *J. Colloid Interface Sci.*, 1982, **85**, 463–478.